Fully Alloyed Ag/Au Nanospheres: Combining the Plasmonic Property of Ag with the Stability of Au

5 AUTHORS, INCLUDING:

Chuanbo Gao
Xi'an Jiaotong University
34 PUBLICATIONS   **872** CITATIONS

SEE PROFILE

Yongxing Hu
C3Nano
47 PUBLICATIONS   **2,832** CITATIONS

SEE PROFILE

Miaofang Chi
Oak Ridge National Laboratory
149 PUBLICATIONS   **4,653** CITATIONS

SEE PROFILE

Yadong Yin
University of California, Riverside
269 PUBLICATIONS   **23,241** CITATIONS

SEE PROFILE

Fully Alloyed Ag/Au Nanospheres: Combining the Plasmonic Property of Ag with the Stability of Au

Chuanbo Gao,*,[†,‡] Yongxing Hu,[§] Mingsheng Wang,[‡] Miaofang Chi,[∥] and Yadong Yin*,[‡]

[†]Center for Materials Chemistry, Frontier Institute of Science and Technology, Xi'an Jiaotong University, Xi'an, Shaanxi 710054, China

[‡]Department of Chemistry, University of California, Riverside, California 92521, United States

[§]Center for Nanoscale Materials, Argonne National Laboratory, 9700 South Cass Avenue, Argonne, Illinois 60439, United States

[∥]Center for Nanophase Materials Sciences, Oak Ridge National Laboratory, Oak Ridge, Tennessee 37831, United States

Ⓢ *Supporting Information*

ABSTRACT: We report that fully alloyed Ag/Au nanospheres with high compositional homogeneity ensured by annealing at elevated temperatures show large extinction cross sections, extremely narrow bandwidths, and remarkable stability in harsh chemical environments. Nanostructures of Ag are known to have much stronger surface plasmon resonance than Au, but their applications in many areas have been very limited by their poor chemical stability against nonideal chemical environments. Here we address this issue by producing fully alloyed Ag/Au nanospheres through a surface-protected annealing process. A critical temperature has been found to be around 930 °C, below which the resulting alloy nanospheres, although significantly more stable than pure silver nanoparticles, can still gradually decay upon extended exposure to a harsh etchant. Nanospheres annealed above the critical temperature show a homogeneous distribution of Ag and Au, minimal crystallographic defects, and the absence of structural and compositional interfaces, which account for the extremely narrow bandwidths of the surface plasmon resonance and may enable many plasmonic applications with high performance and long lifetime, especially for those involving corrosive species.
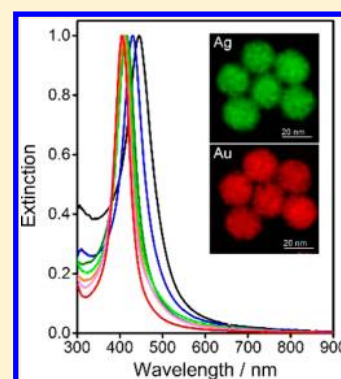
■ INTRODUCTION

Surface plasmon resonance (SPR) of metal nanoparticles has opened up emerging opportunities in a broad range of applications, such as chemical or biomolecular sensing, imaging, photothermal therapy of tumors, and sensitization in solar energy harvesting.[1−3] These applications rely on large extinction cross sections of the nanoparticles for improved performance and high chemical stability for extended lifetimes, which are highly desired and have been the goal of long-term exploration.[4−6] It has been recognized that the plasmonic property of metal nanoparticles is largely dependent on their intrinsic dielectric constant apart from their size, anisotropy, and properties of the medium, and therefore, a silver-rich composition is essential among various metals for supporting strong surface plasmon polarization modes across the visible range of the electromagnetic spectrum because it has the highest plasmonic activity in terms of quality factor, which arises from its appropriate electronic structure and thus dielectric function.[7−10] Unfortunately, the excellent plasmonic property of Ag nanostructures has not been fully utilized in practical applications because of their poor chemical and structural stability against nonideal chemical environments. To this end, methods have been developed in earlier studies to stabilize Ag nanostructures for potential plasmonic applications, typically through coverage of an inorganic layer or a self-

assembled organic monolayer (SAM) over a Ag nanoparticle, giving rise to a core/shell nanostructure.[5,6,11] However, the overlayer is often vulnerable to external etchants, and prolonged exposure to them can still easily cause a loss of the stability of the Ag nanoparticles. In addition, the layer covering the Ag nanostructure may often diminish the plasmonic activity of the original Ag nanostructure. Therefore, it becomes crucial to devise alternative strategies for achieving Ag-rich nanostructures with high stability and excellent plasmonic properties, for example, by alloying Ag with a chemically inert plasmonic metal such as gold.[12,13]

Conventionally, Ag/Au alloy nanoparticles are synthesized by coreduction of a mixture of Ag and Au precursors, for example, $HAuCl_4$ and $AgNO_3$.[13−19] Since the formation of Ag/Au alloy nanoparticles depends on the reduction rates of the respective precursors, it is difficult to achieve compositional homogeneity of Ag and Au across an alloy nanoparticle, as indicated by more close investigations that have revealed stepwise reduction and growth of the metals.[20] The homogeneity can be enhanced through interdiffusion of Ag and Au into one another by means of annealing at elevated temperatures,[21,22] laser irradiation,[23−25] or ultrasonic treatment.[26] However, the energy input into the

nanoparticles is still limited in these cases. For example, the temperature of annealing is limited to the decomposition temperature of their capping agents (oleylamine, etc.) to ensure the stability of the nanoparticle colloid, which impedes efficient interdiffusion and complete alloying of Ag and Au.[21] Alloy nanostructures of Ag and Au may also arise from galvanic replacement of a Ag nanoparticle with a salt of Au, which however often leads to the formation of nanocages or nanoframes as well as a lack of control over the ratio and the distribution of the Ag and Au components.[27−29]

Compositional inhomogeneity is expected to be present in the Ag/Au alloy nanoparticles produced by the state-of-the-art synthesis strategies, with the Ag/Au ratio varying from one domain to another. On one hand, as the stability of the alloy nanoparticles heavily relies on the Ag/Au ratio, corrosion easily starts from unstable domains upon exposure to an etchant, and the stability in both morphology and optical properties of the alloy nanoparticles is significantly reduced as a result. On the other hand, the compositional domains create interfaces that may also affect the plasmonic property of the nanoparticles. According to Mie theory, crystalline grain boundaries in a noble-metal nanoparticle play a critical role in the damping of surface plasmons and significantly enhance scattering events.[30] In a similar manner, damping of surface plasmons can also result from interfaces between domains of different compositions and thus different dielectric properties in the Ag/Au alloy nanoparticles, producing broad bandwidths of the extinction spectrum as observed in most literature reports,[15,22,31] which add additional limitations to many of their plasmon-based applications.

Here we report that an excellent plasmonic property comparable to that of pure Ag nanoparticles and significantly enhanced chemical stability can be achieved in fully alloyed Ag/Au nanospheres. Our synthesis strategy is based on interfacial atomic diffusion of Ag and Au in a Au@Ag core/shell nanoparticle.[32] To ensure complete alloying of Ag and Au, the diffusion efficiency of the Ag and Au atoms has been significantly accelerated by annealing the core/shell nanoparticles at a temperature of ~1000 °C, which is close to their respective melting points (bulk Au, 1064.2 °C; Ag, 961.8 °C) and is unprecedentedly high in the synthesis of Ag/Au alloy nanoparticles. It is expected that an atomically homogeneous distribution of Ag and Au is conveniently established at this temperature. As no conventional surfactants can survive at such a high temperature, a layer of silica is coated on the core/shell nanoparticles prior to their annealing to serve as a high-temperature-resistant "surfactant" to prevent interparticle agglomerations, which enables retention of the size features of the nanoparticles and eventual obtainment of monodisperse fully alloyed Ag/Au nanoparticles as a well-dispersed colloid for potential plasmon-based applications.

■ EXPERIMENTAL SECTION

Synthesis of Au Nanoparticles (~15 nm). A seeded-growth route was chosen for large-scale synthesis of Au nanoparticles of a predetermined size.[33] Typically, a growth solution was prepared by incorporating 12 mL of poly(vinylpyrrolidone) (PVP) (5 wt %, M_w = 10 000), 6 mL of ascorbic acid (0.1 M), 4.5 mL of potassium iodide (0.2 M), and 1.8 mL of $HAuCl_4$ (0.254 M) in 60 mL of H_2O. Into this solution was quickly injected under stirring 48 mL of a seed solution (3.5 nm Au nanoparticles), which was prepared following a literature report.[34] After 10 min, the Au nanoparticles formed were collected by centrifugation and redispersed in 120 mL of H_2O as a stock solution.

Synthesis of Au@Ag Core/Shell Nanoparticles. In a typical synthesis of Au@Ag core/shell nanoparticles (Ag/Au = 5), 4 mL of the Au nanoparticle (~15 nm) stock solution was mixed with 15.5 mL of H_2O, 4.5 mL of PVP (5 wt %, M_w = 10 000), 15 mL of acetonitrile, and 0.91 mL of ascorbic acid (0.1 M), after which 0.76 mL of $AgNO_3$ solution (0.1 M) was injected at a rate of 0.05 mL/min. After 10 min, the Au@Ag nanoparticles were collected in 12 mL of H_2O.

Silica Coating. To the 12 mL of the Au@Ag core/shell nanoparticle solution was slowly added 4 mL of an ethanolic solution of 16-mercaptohexadecanoic acid (MHA) (1 mM), and the resultant solution was then mixed with 76 mL of ethanol. After that, 4 mL of diethylamine and 160 μL of tetraethyl orthosilicate (TEOS) were added in sequence under stirring, and the reaction was allowed to proceed for 90 min. This afforded a colloid of Au@Ag@SiO₂ nanoparticles after centrifugation and redispersion.

Annealing and Silica Removal. In a standard process, the Au@Ag@SiO₂ nanoparticles were dried and annealed at 1000 °C for 6 h in a tube furnace in a nitrogen atmosphere for effective alloying of the Ag and Au. The sample after annealing was redispersed by sonication in 40 mL of a water solution containing 1.25 wt % PVP (M_w = 10 000), 50 mM diethylamine, and 5 mM NaOH, and the resulting dispersion was refluxed at 100 °C for 1 h in a nitrogen atmosphere to ensure complete removal of the silica shell and restabilization of the alloy nanospheres with PVP. Diethylamine was employed to help prevent potential etching of surface Ag species because of its capping effect to Ag.[6,36] Pure Ag/Au alloy nanospheres were then collected by centrifugation and redispersed in 8 mL of H_2O for future use.

Detection of Benzidine from an Artificial Industrial Wastewater by SERS. In a typical process, 20 μL of a nanoparticle solution was dried on a glass substrate in vacuum, which was then soaked in an artificial industrial wastewater (2.4 vol % MeOH, 0.5 μM benzidine, 2 wt % NaCl, 1 mM H_2O_2, pH 10) for different lengths of time (10−60 min). The glass substrate was then washed, dried in vacuum, and subjected to surface-enhanced Raman spectroscopy (SERS) with spectra recorded for evaluation of the enhancement rendered by different noble-metal nanoparticles of the same size and concentration. As all of the nanoparticles investigated in this study exhibit strong coupling at a wavelength of 633 nm after being deposited on glass substrates (Figure S9 in the Supporting Information), the Raman signals were excited with a laser at this wavelength, and the scattering spectra were recorded over the range of 500−2000 cm⁻¹ with an acquisition time of 10 s for each spectrum.

■ RESULTS AND DISCUSSION

In a typical synthesis, a one-step coordination-based method was employed to afford monodisperse Au nanoparticles of a designated size in a large quantity as a starting material.[33,35] Uniform coating of Ag on the Au nanoparticles was then achieved through seeded growth, with self-nucleation of Ag being suppressed in the presence of acetonitrile.[36−38] The exclusive Au@Ag core/shell nanoparticles obtained were transferred to ethanol with the aid of MHA and then coated with a silica layer by a sol−gel reaction of TEOS with a tertiary amine as a catalyst to avoid possible etching of Ag. The materials were then collected, annealed at 1000 °C in a nitrogen atmosphere, treated with a solution of sodium hydroxide (NaOH) to remove the silica, and transferred to water to form a stable colloid of the Ag/Au alloy nanospheres as a final product.

Figure 1 shows transmission electron microscopy (TEM) characterization of the Ag/Au alloy nanospheres and their synthesis intermediates (nominal Ag/Au ratio = 5). After seeded growth of Ag over 15 nm Au nanoparticles (Figure 1a), Au@Ag core/shell nanostructures were formed in high yield, as indicated by a clear Z-contrast boundary in the TEM image (Figure 1b) and unambiguously confirmed by dark-field scanning transmission electron microscopy (DF-STEM) and
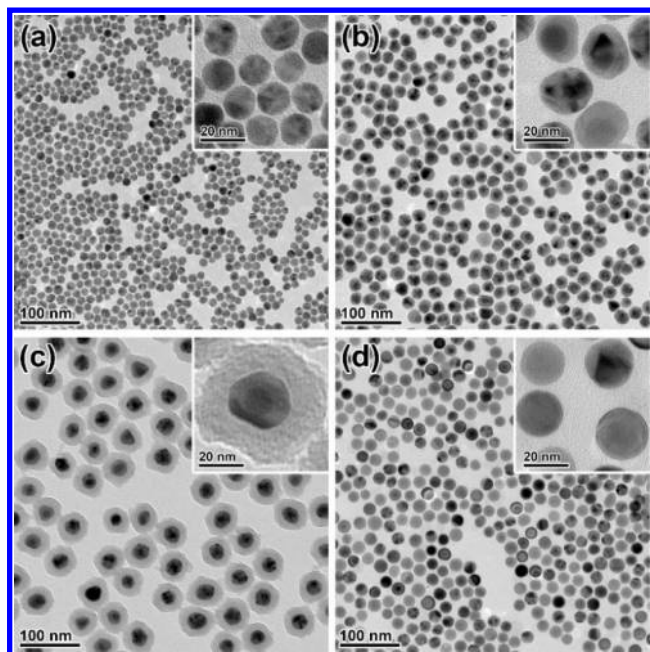
Figure 1. TEM images of (a) Au nanoparticles, (b) Au@Ag core/shell nanoparticles, (c) Au@Ag@SiO$_2$ nanoparticles, and (d) Ag/Au alloy nanospheres obtained from a typical synthesis of Ag/Au alloy nanospheres (Ag/Au = 5).

energy-dispersive X-ray spectroscopy (EDX) elemental mapping (Figure S2). An increase in particle size to 22 nm and lattice matching between the Au core and the Ag shell due to an epitaxial growth mechanism were also observed (Figure 2a).
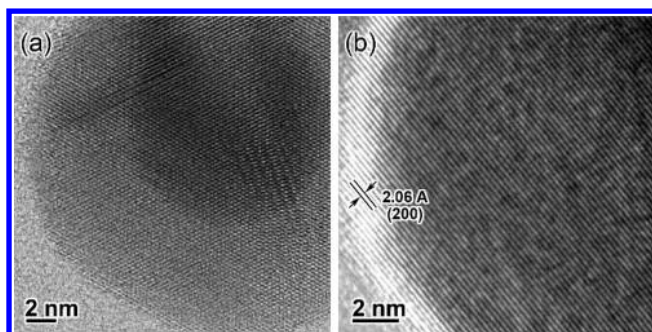

Figure 2. (a) Bright-field STEM image of a Au@Ag core/shell nanosphere (Ag/Au = 5), demonstrating epitaxial growth of Ag on the Au core. (b) HRTEM image of the Ag/Au alloy nanosphere (Ag/Au = 5), showing the single-crystalline nature of the particle.

After silica coating, an amorphous silica layer with a thickness of ~15 nm was formed on the surface of the metal nanoparticles without discernible etching of Ag, which was prevented by the use of a tertiary amine instead of commonly used ammonia as a catalyst (Figure 1c). After high-temperature annealing at 1000 °C and silica etching, a colloid of uniform 22 nm Ag/Au alloy nanoparticles was obtained (Figures 1d and S1). The absence of large particles confirms the effective protection by the silica layer at the elevated temperature. The high-temperature annealing was found to affect a number of features of the metal nanoparticles, including their morphology, structure, and composition. First, the metal nanoparticles after annealing were nearly perfect nanospheres (Figures 1d and S3), in contrast to the irregular shapes of the original core/shell

ones (Figure 1c), which can be attributed to (*i*) the reshaping of the metal nanospheres due to the enhanced mobility of the metal atoms at high temperature and (*ii*) the high glass-transition temperature of silica, which ensured that it remained robust at a high temperature to maintain continuous coating of the metal nanospheres and allow the reshaping of the metal particles. Second, high-resolution TEM (HRTEM) (Figures 2b and S3) showed that the alloy nanospheres after annealing were single crystals (although a few planar defects could occasionally be observed), in contrast to the original core/shell ones, which were basically polycrystalline (Figure 1a−c). This can be ascribed to a release of crystallographic defects as a result of the high atomic mobility of the metals at high temperature, which represents an effective pathway for achieving single-crystalline metal nanoparticles. Most importantly, the high-temperature annealing greatly increased the diffusion rates of Ag and Au atoms and enabled complete mixing of the two metals on the atomic scale, leading to fully alloyed nanospheres, as evidenced by the complete overlap of the elemental distributions of Ag and Au in EDX mapping (Figure 3).
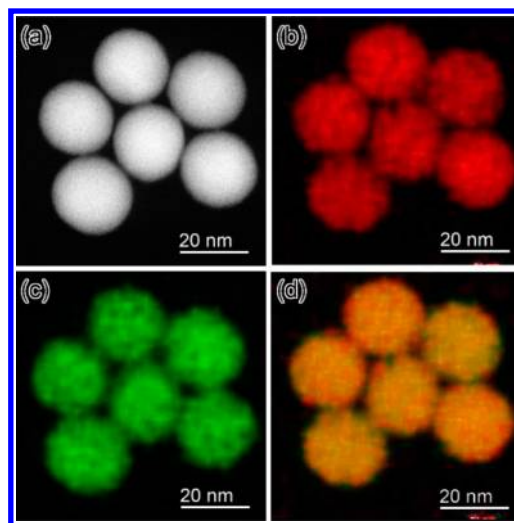

Figure 3. Elemental analysis of the Ag/Au alloy nanospheres (Ag/Au = 5): (a) DF-STEM image; (b, c) EDX elemental maps of Au and Ag, respectively; (d) merged image of (b) and (c).

The spectral properties of the Ag/Au alloy nanospheres and their synthesis intermediates were further investigated (Figure 4). When a thin layer of Ag was coated on the Au nanoparticles, a peak arose that is analogous to a combination of the spectra from the respective Au and Ag, making the overall spectrum a relatively broad one (Figure 4a). The broadening can be attributed to the scattering effect of the Ag−Au boundary on the conduction electrons, which leads to damping of the surface plasmons.[39] The abrupt change of the spectral feature suggests that the optical response of a noble-metal nanoparticle is very sensitive to its outer-shell composition.[7,40] Further coating of a thick Ag layer produced a Ag-like resonance at a wavelength of ~410 nm with a minor yet continuous red shift arising from the increased particle size. After silica coating, annealing, and silica removal, the resultant Ag/Au alloy nanospheres showed a resonance peak that is nearly symmetric and much narrower than the peak of the core/shell nanoparticles (Figure 4b). Apparently, the monodispersity and the uniform spherical shape of the Ag/Au alloy nanospheres contribute to their distinguishing spectral features, including their narrow
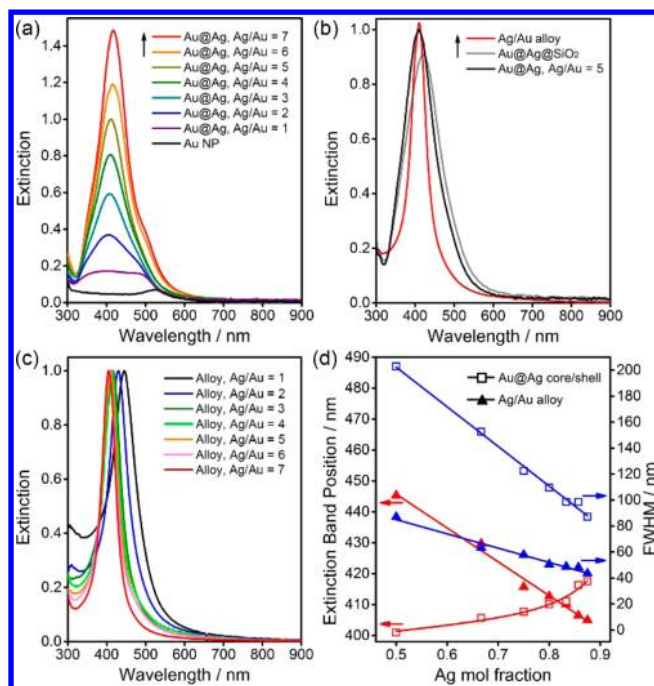
Figure 4. Spectroscopic study of the core/shell and alloy nanoparticles. (a) Optical evolution of the Au@Ag core/shell nanoparticles during seeded growth of Ag on Au nanoparticles. The spectra have been normalized relative to the maximum of the Au@Ag (Ag/Au = 5) spectrum. (b) Optical evolution from Au@Ag (Ag/Au = 5) core/shell nanoparticles to Ag/Au alloy nanospheres. The spectra have been normalized relative to the spectral maximum of the Au@Ag core/shell nanoparticles. (c) UV−vis extinction spectra of Ag/Au alloy nanospheres with different Ag/Au ratios, which have been normalized relative to their respective maxima. (d) Dependence of the band position and full-width at half-maximum (FWHM) of extinction peaks of the Au@Ag core/shell and Ag/Au alloy nanoparticles on the Ag mole fraction.

bandwidth. More importantly, the alloy nanospheres are different from the core/shell ones in that (*i*) they are single crystals containing no crystallographic defects and (*ii*) the Ag and Au elements are homogeneously distributed without compositional interfaces over the whole nanoparticle. The effect of the former on the bandwidth of the resonance peaks has been demonstrated in the literature[30] and was confirmed in our experiment by an investigation of the spectral change of the Ag nanospheres after removal of crystallographic defects by high-temperature annealing relative to the as-synthesized ones (Figure S6). However, the effect of the latter on the bandwidth has not been reported to date in literature-related alloy nanoparticles. Conventionally synthesized Ag/Au alloy nanoparticles usually show a nonsymmetric resonance peak as a result of strong coupling of the collective oscillation of conduction electrons to the interband transitions,[14,17,18] which is a typical character of Au nanoparticles, indicating the presence of Au-rich domains in the alloy nanoparticles and thus poor compositional homogeneity of the Ag and Au elements. It also explains that these alloy nanoparticles usually show broad extinction peaks as a result of scattering of the conduction electrons at the compositional interfaces, in a way similar to the scattering events at a Ag−Au boundary in a Au@Ag core/shell nanoparticle, which produces a broad resonance peak as well.[38] Therefore, the narrow and symmetric resonance peak of the Ag/Au alloy nanospheres synthesized by the high-

temperature annealing approach can be attributed not only to the removal of crystallographic defects but more importantly to the elimination of compositional interfaces, suggesting that fully alloyed nanoparticles were prepared as such with an electronic structure that was homogeneously modified during alloying. Additionally, the extinction efficiency of the alloy nanoparticles is very close to that of the Ag-like Au@Ag core/shell nanoparticles (Figure 4b), indicating that the plasmonic property of the alloy nanoparticles is dominated by Ag, which together with the narrow bandwidth enables high performance in many plasmon-based applications.

The Ag/Au ratio in the alloy nanospheres can easily be tuned by controlling the amounts of respective precursors in the synthesis (Figures 4c and S3−S5), and their plasmonic properties are plotted in Figure 4d. UV−vis spectroscopy showed that the extinction bands underwent a blue shift with an increase in the mole fraction of Ag despite the slightly increased particle size, which is supposed to result in a red shift of the bands for particles of the same composition. Therefore, the band shift of the alloy nanospheres is dominated by the Ag/Au ratio, consistent with earlier reports.[14] The bandwidth of the alloy nanospheres was also found to exhibit a linear relationship with the mole fraction of Ag in the alloy nanospheres and to be much narrower than that of their core/shell counterparts in all cases. These data suggest that the plasmonic properties of the alloy nanospheres can be delicately manipulated simply by controlling their chemical composition.

The full alloying of Ag and Au not only improves the plasmonic property of the nanospheres but also significantly enhances the chemical stability against corrosive environments, as demonstrated by tests of their stability in a mixed solvent of hydrogen peroxide (H_2O_2) and ammonia (NH_3) (Figure 5).
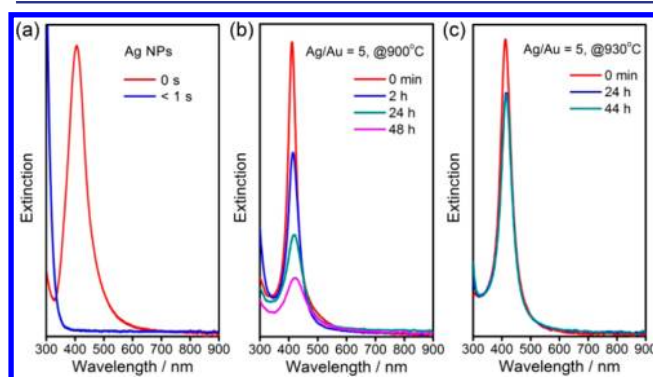

Figure 5. UV−vis spectra showing the chemical stabilities of (a) pure Ag nanoparticles (~22 nm), (b) Ag/Au alloy nanospheres annealed at 900 °C, and (c) Ag/Au alloy nanospheres annealed at 930 °C. The alloy nanospheres had a Ag/Au ratio of 5. The aqueous etchant solution was composed of H_2O_2 (0.5 M), $NH_3 \cdot H_2O$ (0.4 M), and PVP (surfactant, 0.5 wt %, M_w = 10 000). Initial spectra of the nanoparticles (labeled as 0 s or 0 min in the figure) were recorded in the absence of H_2O_2 and $NH_3 \cdot H_2O$, with their volumes made up by water.

The mixed solvent contains both oxidizing and complexing agents and is known to be an excellent etchant to rapidly dissolve metallic Ag (within 1 s; Figure 5a) but not Au (Figure S7). On the other hand, the Ag/Au nanospheres, when alloyed at sufficiently high temperatures, were able to survive in this solution, with only a minor loss in plasmon band intensity even after exposure to the solution for more than 24 h. We found ~930 °C to be a critical temperature below which the resulting

alloy nanospheres, although significantly more stable than pure silver nanoparticles, still gradually decayed upon extended exposure to the etchant, as shown in the case of Ag/Au alloy particles (Ag/Au = 5) annealed at 900 °C (Figure 5b). When annealed at 930 °C, the alloy nanospheres maintained their plasmon band intensity at ~82% of the original value after 24 h of etching, and there was no further decay within an additional 20 h. In order to ensure reproducibility by minimizing the effect of temperature fluctuation during annealing, we used 1000 °C as the standard annealing temperature in this work.

The stability of the alloy nanospheres also depends on the Ag/Au ratio and decreases as the Ag content increases (Figure 6). As an extreme example, in UV−vis extinction Ag/Au alloy
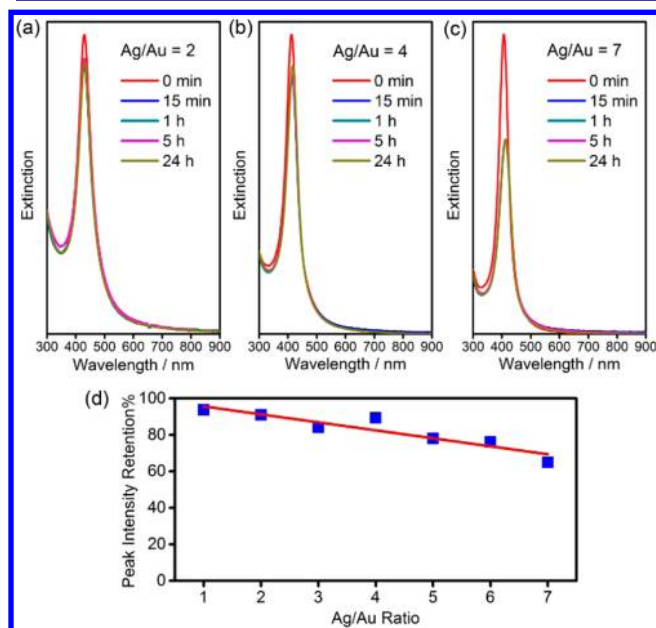

Figure 6. Chemical stability of the Ag/Au alloy nanospheres in an aqueous solution of H_2O_2 and $NH_3 \cdot H_2O$, as indicated by UV−vis spectral changes with time. (a−c) UV−vis spectra of nanospheres with Ag/Au = 2, 4, and 7, respectively, annealed at 1000 °C. (d) Change in the band intensity relative to the initial intensity after 24 h of etching as a function of the Ag/Au ratio.

nanospheres with Ag/Au = 7 retained 65% of their original intensity after 24 h of etching, although the mole fraction of Au in the nanospheres was only 12.5%. A close TEM investigation of a sample after etching (Figure S8) indicated that the alloy nanospheres were mostly retained, although minor etching was observable at certain sites (e.g., at sites having crystallographic defects), which was responsible for the slight decay of the surface plasmon resonance. We therefore conclude that alloy nanospheres synthesized by the high-temperature annealing method possess Ag-like plasmonic property and Au-like stability, which may greatly expand their use in many plasmon-based applications, especially when corrosive reagents are involved.

To demonstrate the significance of stable alloy nanoparticles in practical applications, we devised a SERS-based method to detect molecules of interest from an artificial wastewater (using benzidine, a typical dye precursor, as a model) as a prototype of pollutant control in the dye industry. These industrial wastes basically include salts, oxidants, and acids or bases [simulated in our artificial wastewater with NaCl (2 wt %), H_2O_2 (1 mM), and NaOH (pH 10), respectively]; such conditions are often

too harsh for Ag-based substrates to survive for a reasonably long soaking time, as is typically required for molecular loading in SERS analysis. In these circumstances, the Ag/Au alloy nanoparticles are advantageous in terms of sensitivity and durability of the detection because of their excellent optical property and stability.

Pure Au, Ag and Au@Ag core/shell nanoparticles of the same size and concentration were used as control for comparison. The Raman signals of benzidine from the Ag or Au@Ag substrates were rapidly damped as the soaking time was prolonged for enhanced molecular loading (Figure 7),
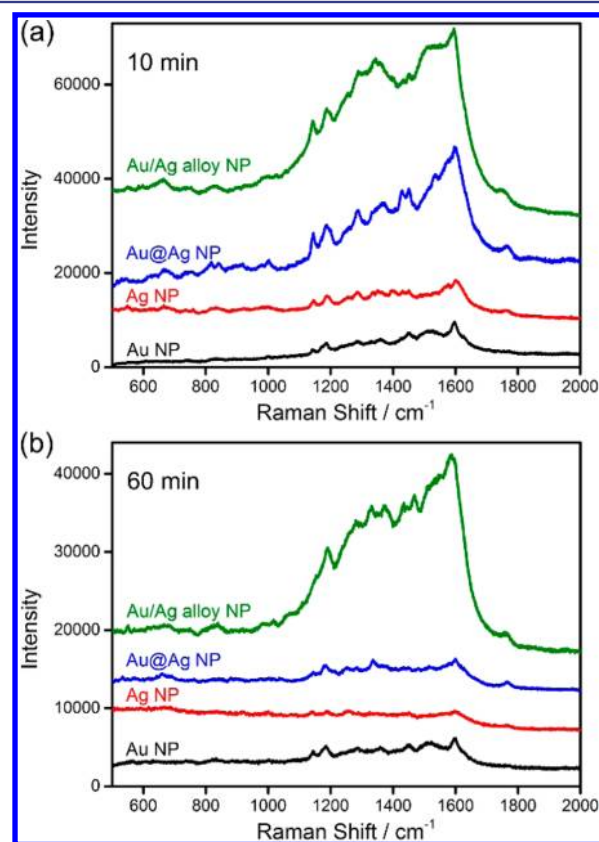

Figure 7. SERS spectra of benzidine (0.5 μM) absorbed from an artificial industrial wastewater (2 wt % NaCl, 1 mM H_2O_2, pH 10) onto nanoparticle-loaded substrates by soaking the substrates in the wastewater for (a) 10 and (b) 60 min. The Ag/Au alloy nanospheres (Ag/Au = 5) showed superior signal enhancement compared with Ag, Au@Ag core/shell, and Au nanoparticles.

which can be attributed to the oxidative etching of Ag in the artificial wastewater. Therefore, it was difficult to obtain stable and strong SERS signals from these substrates, which would introduce much uncertainty and inaccuracy in molecular detection applications. On the other hand, the Au substrate gives stable Raman signals, but the signals were relatively weak because of the small extinction cross sections of the Au nanoparticles. The Raman signals from the substrate of the alloy nanospheres were particularly strong and stable independent of soaking time, confirming its superior signal enhancement in corrosive media as a result of the large extinction cross section (Ag-like) and high stability (Au-like) of the Ag/Au alloy nanospheres.

CONCLUSION

Our study reveals that by a high-temperature annealing approach, unprecedentedly fully alloyed Ag/Au nanospheres that show large cross sections, narrow bandwidths, and high chemical stability can be produced. The results indicate that the high mobility of the metal atoms at high temperatures favors homogeneous distribution of the Ag and Au elements over the whole nanosphere and release of crystallographic defects, removing both structural and compositional interfaces, which accounts for the narrow bandwidth of the surface plasmon resonance. The Ag/Au alloy nanospheres are thus concluded to combine the excellent plasmonic property of Ag and the great stability of Au, which may enable many plasmonic applications with high performance and long lifetime, especially for those involving corrosive species. A sensitive and etching-resistant SERS detection of molecules from an artificial industrial wastewater has been demonstrated in this work, which suggests their promising applications in monitoring of pollution in many natural and industrial contexts. It is also expected that the Ag/Au alloy nanospheres may bring benefits to other applications such as solar energy conversion and bioapplications, where high plasmonic performance and long chemical stability are critically important. The strategy reported here may be extended to other metals such as Pt, Pd, and Ni to produce high-performance catalysts.

ASSOCIATED CONTENT

Ⓢ Supporting Information

Additional experimental details, TEM (STEM) images, and UV−vis spectra. This material is available free of charge via the Internet at http://pubs.acs.org.

AUTHOR INFORMATION

Corresponding Authors
gaochuanbo@mail.xjtu.edu.cn
yadong.yin@ucr.edu

Notes

The authors declare no competing financial interest.

ACKNOWLEDGMENTS

REFERENCES

(1) Daniel, M.-C.; Astruc, D. *Chem. Rev.* **2004**, *104*, 293−346.
(2) Sperling, R. A.; Rivera Gil, P.; Zhang, F.; Zanella, M.; Parak, W. J. *Chem. Soc. Rev.* **2008**, *37*, 1896−1908.
(3) Linic, S.; Christopher, P.; Ingram, D. B. *Nat. Mater.* **2011**, *10*, 911−921.
(4) Aherne, D.; Charles, D. E.; Brennan-Fournet, M. E.; Kelly, J. M.; Gun'ko, Y. K. *Langmuir* **2009**, *25*, 10165−10173.
(5) Zhang, X.; Zhao, J.; Whitney, A. V.; Elam, J. W.; Van Duyne, R. P. *J. Am. Chem. Soc.* **2006**, *128*, 10304−10309.
(6) Gao, C.; Lu, Z.; Liu, Y.; Zhang, Q.; Chi, M.; Cheng, Q.; Yin, Y. *Angew. Chem., Int. Ed.* **2012**, *51*, 5629−5633.
(7) Lozano, X. L.; Mottet, C.; Weissker, H. C. *J. Phys. Chem. C* **2013**, *117*, 3062−3068.
(8) Rycenga, M.; Cobley, C. M.; Zeng, J.; Li, W.; Moran, C. H.; Zhang, Q.; Qin, D.; Xia, Y. *Chem. Rev.* **2011**, *111*, 3669−3712.
(9) Mulvaney, P. *Langmuir* **1996**, *12*, 788−800.
(10) Link, S.; El-Sayed, M. A. *J. Phys. Chem. B* **1999**, *103*, 8410−8426.
(11) Xue, C.; Chen, X.; Hurst, S. J.; Mirkin, C. A. *Adv. Mater.* **2007**, *19*, 4071−4074.
(12) Cortie, M. B.; McDonagh, A. M. *Chem. Rev.* **2011**, *111*, 3713−3735.
(13) Hostetler, M. J.; Zhong, C.-J.; Yen, B. K. H.; Anderegg, J.; Gross, S. M.; Evans, N. D.; Porter, M.; Murray, R. W. *J. Am. Chem. Soc.* **1998**, *120*, 9396−9397.
(14) Link, S.; Wang, Z. L.; El-Sayed, M. A. *J. Phys. Chem. B* **1999**, *103*, 3529−3533.
(15) Mallin, M. P.; Murphy, C. J. *Nano Lett.* **2002**, *2*, 1235−1237.
(16) Pal, A.; Shah, S.; Devi, S. *Aust. J. Chem.* **2008**, *61*, 66−71.
(17) Russier-Antoine, I.; Bachelier, G.; Sablonière, V.; Duboisset, J.; Benichou, E.; Jonin, C.; Bertorelle, F.; Brevet, P.-F. *Phys. Rev. B* **2008**, *78*, No. 035436.
(18) Wang, C.; Yin, H.; Chan, R.; Peng, S.; Dai, S.; Sun, S. *Chem. Mater.* **2009**, *21*, 433−435.
(19) Shang, L.; Jin, L.; Guo, S.; Zhai, J.; Dong, S. *Langmuir* **2010**, *26*, 6713−6719.
(20) Rodríguez-González, B.; Sánchez-Iglesias, A.; Giersig, M.; Liz-Marzán, L. M. *Faraday Discuss.* **2004**, *125*, 133−144.
(21) Shore, M. S.; Wang, J.; Johnston-Peck, A. C.; Oldenburg, A. L.; Tracy, J. B. *Small* **2011**, *7*, 230−234.
(22) Wang, C.; Peng, S.; Chan, R.; Sun, S. *Small* **2009**, *5*, 567−570.
(23) Hodak, J. H.; Henglein, A.; Giersig, M.; Hartland, G. V. *J. Phys. Chem. B* **2000**, *104*, 11708−11718.
(24) Peng, Z.; Spliethoff, B.; Tesche, B.; Walther, T.; Kleinermanns, K. *J. Phys. Chem. B* **2006**, *110*, 2549−2554.
(25) Wang, X.; Zhang, Z.; Hartland, G. V. *J. Phys. Chem. B* **2005**, *109*, 20324−20330.
(26) Radziuk, D. V.; Zhang, W.; Shchukin, D.; Mohwald, H. *Small* **2010**, *6*, 545−553.
(27) Skrabalak, S. E.; Chen, J.; Sun, Y.; Lu, X.; Au, L.; Cobley, C. M.; Xia, Y. *Acc. Chem. Res.* **2008**, *41*, 1587−1595.
(28) Zhang, Q.; Lee, J. Y.; Yang, J.; Boothroyd, C.; Zhang, J. *Nanotechnology* **2007**, *18*, No. 245605.
(29) Zhang, Q.; Xie, J.; Liang, J.; Lee, J. Y. *Adv. Funct. Mater.* **2009**, *19*, 1387−1398.
(30) Tang, Y.; Ouyang, M. *Nat. Mater.* **2007**, *6*, 754−759.
(31) Wilcoxon, J. *J. Phys. Chem. B* **2009**, *113*, 2647−2656.
(32) Shibata, T.; Bunker, B. A.; Zhang, Z.; Meisel, D.; Vardeman, C. F.; Gezelter, J. D. *J. Am. Chem. Soc.* **2002**, *124*, 11989−11996.
(33) Gao, C.; Vuong, J.; Zhang, Q.; Liu, Y.; Yin, Y. *Nanoscale* **2012**, *4*, 2875−2878.
(34) Jana, N. R.; Gearheart, L.; Murphy, C. J. *Langmuir* **2001**, *17*, 6782−6786.
(35) Gao, C.; Goebl, J.; Yin, Y. *J. Mater. Chem. C* **2013**, *1*, 3898−3909.
(36) Gao, C.; Zhang, Q.; Lu, Z.; Yin, Y. *J. Am. Chem. Soc.* **2011**, *133*, 19706−19709.
(37) Liu, X.; Yin, Y.; Gao, C. *Langmuir* **2013**, *29*, 10559−10565.
(38) Liu, X.; Li, L.; Yang, Y.; Yin, Y.; Gao, C. *Nanoscale* **2014**, *6*, 4513−4516.
(39) Liu, M.; Guyot-Sionnest, P. *J. Phys. Chem. B* **2004**, *108*, 5882−5888.
(40) Jiang, R.; Chen, H.; Shao, L.; Li, Q.; Wang, J. *Adv. Mater.* **2012**, *24*, OP200−OP207.